Syk Tyrosine Kinase Is Linked to Cell Motility and Progression in Squamous Cell Carcinomas of the Head and Neck

Sutima Luangdilok,[1] Carol Box,[1] Lisa Patterson,[1] William Court,[1] Kevin Harrington,[2,3] Lisa Pitkin,[3] Peter Rhŷs-Evans,[3] Pornchai O-charoenrat,[4] and Suzanne Eccles[1]

[1]Tumour Biology and Metastasis Team, Cancer Research UK Centre for Cancer Therapeutics, The Institute of Cancer Research, McElwain Laboratories, Sutton, Surrey, United Kingdom; [2]Targeted Therapy Team, Section of Cell and Molecular Biology, Chester Beatty Laboratories; [3]Head and Neck Unit, Royal Marsden Hospital, London, United Kingdom; and [4]Division of Head and Neck Surgery, Department of Surgery, Siriraj Hospital Medical School, Bangkok, Thailand

Abstract

Syk, a non–receptor tyrosine kinase, is an important component of immunoreceptor signaling in hematopoietic cells. It has been implicated in key regulatory pathways including phosphoinositide 3-kinase and phospholipase Cγ (PLCγ) activation in B cells and integrin signaling in platelets and bronchial epithelial cells. Recently, potential roles in cancer have been reported. In breast cancers, reduced Syk expression was associated with invasion, and its overexpression in cell lines was shown to inhibit cell motility. In contrast, Syk has been shown to mediate chemomigration in nasopharyngeal carcinoma cells. Its role in squamous cell carcinomas of the head and neck (SCCHN) has not yet been investigated. Syk mRNA and protein expression was detected in 6 of 10 SCCHN cell lines. When Syk was transfected into Syk-negative cells (SIHN-011A), chemomigration was enhanced *in vitro* and this was associated with activation of PLCγ1. Conversely, abrogation of Syk activity by pharmacologic inhibition or small interfering RNA in HN6 cells with high levels of endogenous expression inhibited migration, haptotaxis, and engagement with matrix proteins; this was accompanied by decreased levels of phosphorylated AKT. Similar effects were seen in Syk-positive CAL 27 cells but not in Syk-negative SIHN-011A cells. Immunoprecipitation suggested co-association of Syk with epidermal growth factor receptor and GRB-2. Syk expression in SCCHN patient tissues was examined by semiquantitative real-time PCR (n = 45) and immunohistochemistry (n = 38) in two independent cohorts. Higher levels of Syk expression were observed in tumors and lymph node metastases relative to normal tissues. High Syk expression significantly correlated with worse survival and may be of prognostic value in SCCHN due to its potential role in cell migration and invasion. [Cancer Res 2007;67(16):7907–16]

Introduction

Syk is a member of the Syk/ZAP family of non–receptor tyrosine kinases whose two isoforms consist of two tandem NH_2-terminal SH2 domains and a COOH-terminal kinase domain (ref. 1; Fig. 1*A*). Syk is abundant in B lymphocytes and expressed at lower levels in immature T cells, mast cells, and platelets. In addition, Syk has been detected in fibroblasts (2, 3), epithelial cells (4), and breast tissues (5). In endothelial cells, it plays a key role in proliferation, migration, and developmental angiogenesis/lymphangiogenesis (6–8). Syk is essential for lymphocyte development and antigen receptor signaling (1). Syk interacts with the immunoreceptor tyrosine-based activation motifs of immunoglobulin α, T-cell receptor ζ, CD3ε, and FcεRI, coupling immune receptors to multiple downstream signaling events including activation of phospholipase Cγ (PLCγ), mobilization of calcium from intracellular stores, and activation of Ras/extracellular signal–regulated kinase (ERK), phosphoinositide 3-kinase (PI3K), and nuclear factor-κB pathways (9, 10).

Syk is also essential in mast cell signaling downstream of FcεRI aggregation leading to degranulation and histamine release (11). Important downstream targets of Syk in mast cells include PLCγ1, whose activation leads to intracellular calcium flux and NFAT and Vav activation (1, 12). Platelet spreading on extracellular matrix requires sequential activation of Src and Syk (13), and in bronchial epithelial cells, Syk is involved in a β_1-integrin signaling pathway (14).

Syk has not been widely studied in the field of cancer, but two recent publications are of interest. In breast cancers, reduced Syk expression was associated with invasion and its overexpression in cell lines was shown to inhibit cell migration (5). In contrast, Syk mediates cell migration in nasopharyngeal carcinoma (15). The role of Syk in squamous cell carcinomas of the head and neck (SCCHN) has not been investigated.

SCCHN are locally invasive cancers that frequently disseminate to lymph nodes; this factor is the most important determinant of patient prognosis. With better local control, there has been an increase in the detection of distant metastases (16). Epidermal growth factor (EGF) receptor (EGFR), expressed in >90% of these cancers (17), is the key molecular driver of oncogenesis and progression. Activated EGFR is linked to metastasis by its ability to induce a motile and invasive phenotype (16, 18, 19). Downstream of EGFR, PI3K and PLCγ1 are important and complementary regulators of cell motility and migration. Recently, an interaction between Syk and EGFR has been reported in mammary epithelial cells (20). Given the possible interactions of Syk with EGFR, PI3K (21), and PLCγ1 (22), we reasoned that Syk might modulate key cellular functions in SCCHN. The present study aimed to explore the role of Syk in SCCHN by modulating its expression or activity and determining its effects on malignant cell behavior. Syk expression in clinical SCCHN samples was also determined in pilot studies to seek preliminary evidence of possible clinical significance.

Note: Supplementary data for this article are available at Cancer Research Online (http://cancerres.aacrjournals.org/).

S. Luangdilok and C. Box contributed equally to this work.

Requests for reprints: Suzanne Eccles, McElwain Laboratories, The Institute of Cancer Research, 15 Cotswold Road, Belmont, Sutton, Surrey SM2 5NG, United Kingdom. Phone: 44-20-8722-4210; Fax: 44-20-8722-4134; E-mail: Sue.Eccles@icr.ac.uk.

doi:10.1158/0008-5472.CAN-07-0331

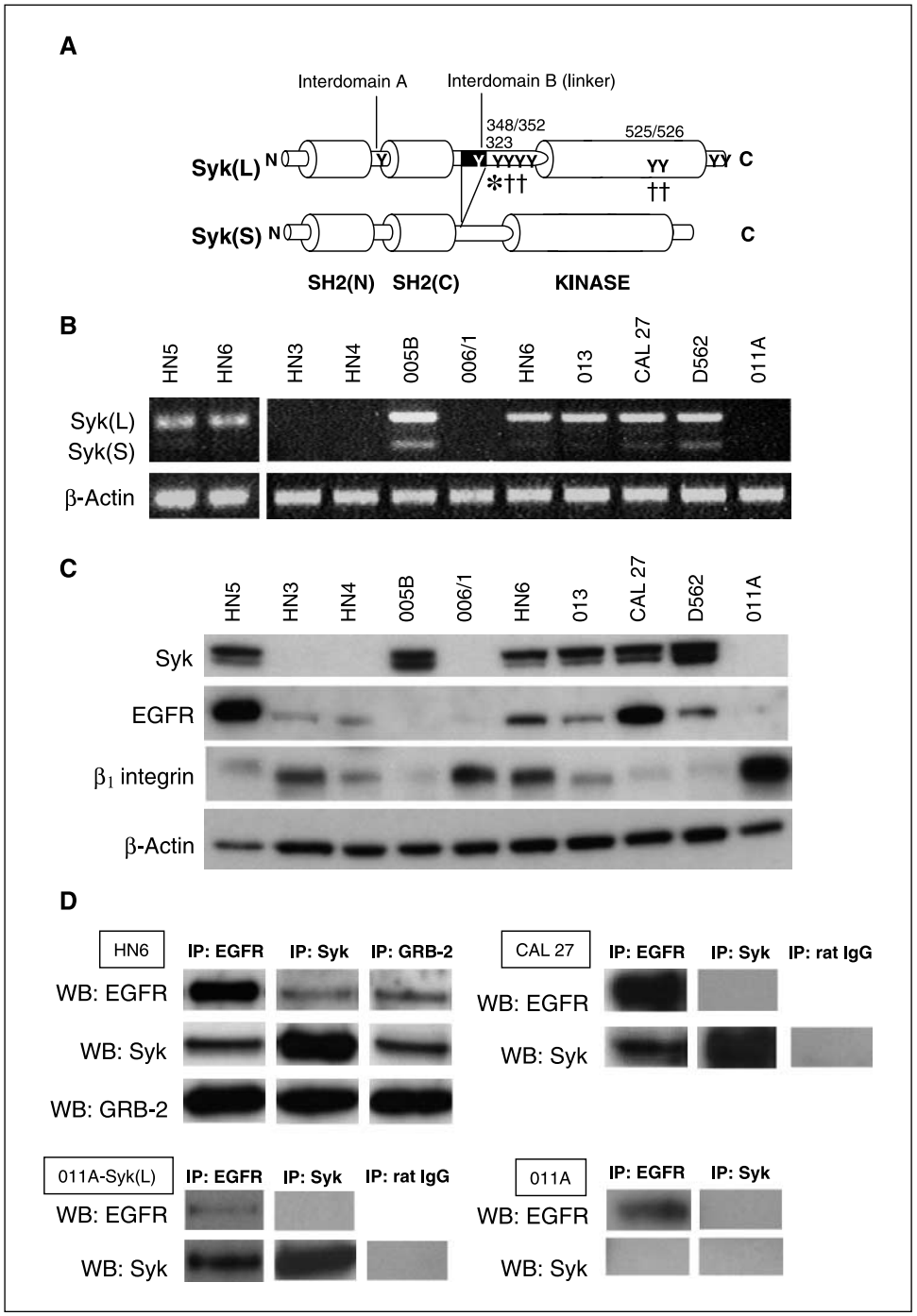

Figure 1. Syk is expressed in SCCHN cells and co-associates with EGFR and GRB-2. *A,* schematic representation of domain structure of human Syk splice variants, Syk(L) and Syk(S), showing positions of key regulatory tyrosine residues (adapted from ref. 1). *, phosphotyrosine PI3K p85 binding site; †, PLCγ binding sites. *B,* SCCHN RNA was converted to cDNA and RT-PCR was used to evaluate Syk expression. *C,* SCCHN cell lysates were analyzed by Western blot for expression of Syk, EGFR, and β_1 integrin. β-Actin was used as a loading control. *D,* Syk-positive HN6 (*top left*), CAL 27 (*top right*), 011A-Syk(L) (*bottom left*), or Syk-negative 011A (*bottom right*) cell lysates were immunoprecipitated with antibodies to EGFR, Syk, GRB-2, or rat immunoglobulin G (*IgG*) and blotted with antibodies to EGFR, Syk, or GRB-2.

Materials and Methods

Cell culture and reagents. SCCHN cell lines were obtained from American Type Culture Collection (CAL 27 and Detroit 562), the Ludwig Institute (LICR-LON-HN3, LICR-LON-HN4, LICR-LON-HN5, and LICR-LON-HN6), or SCCHN patients at the Royal Marsden Hospital, London (SIHN-005B, SIHN-006/1, SIHN-011A, and SIHN-013; refs. 23, 24). Cells were grown in DMEM/10% FCS at 37°C. Piceatannol was from Tocris Bioscience and BAY 61-3606 from Calbiochem. Antibodies used for Western blotting, immunoprecipitation, and immunohistochemistry are listed in Supplementary data.

Transfection of Syk cDNA. Syk plasmids including pcDNA3.1-Syk(L) and pcDNA3.1-Syk(S) were a generous gift from Dr. Jiale Dai. Syk(L) or its alternative spliced variant Syk(S) was transfected into SIHN-011A cells using Lipofectamine 2000 (Invitrogen) according to the manufacturer's instructions and selected with 1,100 μg/mL G418. Clones were isolated, expanded, and screened for protein expression by Western blotting.

Small interfering RNA treatment. Cells were transfected with small interfering RNA (siRNA; 200 μmol/L final concentration) using Lipofectamine 2000 (Invitrogen) according to the manufacturer's instructions. SiRNA to Syk was purchased from Dharmacon. The negative siRNA control contained two inverted central nucleotides and a National Center for Biotechnology Information BLAST search ensured that sequences did not match any human RNA sequences: Syk siRNA, GAACUGGGCUCUG-GUAAUU; inverted siRNA, GAACUGGCGUCUGGUAAUU.

Reverse transcription-PCR. Total RNA was extracted using an RNeasy Mini Kit (Qiagen) and converted to cDNA using Omniscript reverse

transcription kit (Qiagen) according to the manufacturer's instructions. Syk and β-actin control primer sequences (25) were Syk forward, 5-TTTTGG-AGGCCGTCCACAAC-3′; Syk reverse, 5′-ATGGGTAGGGCTTCTCTCTG-3′; β-actin forward, 5′-TCGACAACGGCTCCGGCAT-3′; and β-actin reverse, 5′-AAGGTGTGGTGCCAGATTTTC-3′.

Real-time PCR. Real-time PCR with SYBR was done on an Opticon Monitor 2 machine (MJ Research). The DyNAmo SYBR Green qPCR Kit together with 0.5 μmol/L of each primer was used as a master mix (total volume, 20 μL). Cycling conditions were 95°C for 10 min, 35 cycles of 95°C 10 s, 62°C 20 s, and 72°C 20 s. Glyceraldehyde-3-phosphate dehydrogenase (*GAPDH*) was used as a reference gene. A calibrator sample was included in every run and used for normalization of final results. The primers for *Syk* and *GAPDH* were designed to span two introns: Syk forward, 5′-ACTTG-GTCAGCGGGTGGAAT-3′; Syk reverse, 5′-GGGTGCAAGTTCTGGCTCAT-3′; GAPDH forward, 5′-GCACCGTCAAGGCTGAGAAC-3′; and GAPDH reverse, 5′-GTGGTGAAGACGCCAGTGGA-3′.

The data were analyzed and compared using a relative quantification method:

$$R = 2^{-(\Delta\text{CP sample} - \Delta\text{CP calibrator})}$$

where R is relative amount of Syk relative to GAPDH; ΔCP = cycle threshold of Syk − cycle threshold of GAPDH.

Western blotting. Cells were lysed with lysis buffer [150 mmol/L NaCl, 1 mmol/L EDTA, 50 mmol/L Tris, 1% Triton X-100, 1 nmol/L NaF, 1 mmol/L Na_3VO_4, 10 μg/mL Na-p-tosyl-L-lysine chloromethyl ketone (hydrochloride), 1 mmol/L DTT, 5 μmol/L fenvalerate, 5 μmol/L potassium bisperoxo (1,10-phenanthroline) oxovanadate (V), 1 mmol/L phenylmethylsulfonyl fluoride, protease inhibitor cocktail, phosphatase inhibitor cocktail I and II (Sigma)]. Lysates were incubated on ice for 15 min and spun at 12,000 rpm for 10 min. Protein assays used a detergent-compatible protein assay kit (Bio-Rad) and protein electrophoresis was run using NuPAGE Novex 4% to 12% Bis-Tris gels (Invitrogen) according to the manufacturers' instructions.

Immunoprecipitation. Agarose-conjugated antibody was prepared by adding 60 μL of protein G-agarose bead slurry to 2 μg of antibody. Immunoprecipitation was done by adding cell lysates to the agarose-conjugated antibody complex and incubating at 4°C for 1 h to overnight on a rotator. After extensive washing with lysis buffer, samples were resuspended in reducing sample buffer, boiled for 3 min, centrifuged to pellet the agarose beads, and subjected to Western blotting.

***In vitro* cell proliferation assay.** Methylene blue staining (23) measured cell numbers following transfection. Syk(L)- or Syk(S)-expressing SIHN-011A cells, Neo control, and parental SIHN-011A cells were seeded in 96-well plates at 1,000 per well in DMEM/10% FCS in triplicate. Cells were fixed with glutaraldehyde at 24-h intervals over 4 days. After staining, absorbance was read at 605 nm. Graphs were plotted to indicate cell proliferation over time.

Transwell migration assay. After serum starvation for 24 h, cells were labeled with 3 μmol/L CellTracker Green dye CMFDA (Molecular Probes, Invitrogen) and seeded into the upper chamber of 8-μm-pore Fluoroblok transwell inserts (BD-Falcon) at 2×10^4 to 5×10^4 per well. Five percent FCS was used as a chemoattractant in the lower chamber. Migrated cells were detected using an Olympus IX70 inverted fluorescent microscope and cooled charge-coupled device digital camera with U-MWB filter set cube (Olympus UK Ltd.). Images were captured and cells counted in triplicate wells using Image-Pro Plus software (Media Cybernetics).

Scratch wound haptotaxis assay. Twenty-four-well plates were uncoated or coated with 10 μg/mL collagen I (BD Biosciences) to facilitate rapid cell attachment (26). Cells were seeded at 1×10^5 to 2×10^5 per well and allowed to attach. Compound or vehicle was added and incubated for 1 h, then a straight-line scrape was made in each monolayer using a pipette tip. After two washes to remove detached cells, medium was replaced (with or without compounds as before) and plates were incubated at 37°C for 18 to 24 h until closure of the wound in control monolayers. Wound widths were measured at three positions at time 0 and at assay termination and percent closure was calculated using Image-Pro Plus software.

Cell interactions with Matrigel. Twenty-four-well plates were coated with 300-μL Matrigel (BD Biosciences) and left to gel for 30 min at 37°C. Cells were seeded at 1×10^4 to 6×10^4 per well and, after incubation in piceatannol or vehicle at 37°C for 24 h, images of tubular differentiation were obtained using phase-contrast microscopy. In a second study, cells were pretreated for 1 h with compounds or vehicle, labeled with CellTracker Green dye, and set up as before. Images were obtained after 24 h and the total length of the tubules was measured in each well and expressed as percent control values.

Clinical SCCHN samples. Total RNAs were extracted from frozen sections of SCCHN tumors, nodal metastases, and normal tissues from 45 patients undergoing surgery at Siriraj Hospital, Thailand. Archival paraffin-embedded tumor tissue was also obtained from 38 patients diagnosed with squamous cell carcinoma of the tonsil at St. George's Hospital, London, United Kingdom (in collaboration with Dr. K. Harrington, Royal Marsden Hospital, London, United Kingdom). Study protocols were approved by the appropriate Ethical Committees and all samples were collected with informed consent. The clinicopathologic characteristics of patients are shown in Supplementary Tables S1 and S2.

Immunohistochemistry. Paraffin-embedded tissue sections were dewaxed and antigens were retrieved by microwave treatment in sodium citrate buffer (pH 6.0) and endogenous peroxidase removal. The slides were blocked and incubated overnight with Syk antibody (4D10; 1:500). Following extensive washing with PBS, slides were incubated with biotinylated antimouse secondary antibody (#715-065-151), 1 μg/mL peroxidase-conjugated streptavidin (#016-030-084), and, finally, in peroxidase substrate solution (3,3′-diaminobenzidine substrate kit for peroxidase, Vector Laboratories) until the desired staining density developed.

Results

Syk is commonly expressed in SCCHN cell lines. Syk expression was determined in a panel of 10 SCCHN cell lines by reverse transcription-PCR (RT-PCR; Fig. 1*B*) and Western blotting (Fig. 1*C*). Six cell lines (HN5, HN6, 013, 005B, CAL 27, and Detroit 562) expressed Syk whereas four cell lines (HN3, HN4, 006/1, and 011A) were negative. Syk(L) and the splice variant Syk(S) (Fig. 1*A*) were detected in all Syk-positive cell lines. There was a weak positive correlation between expression of Syk and EGFR ($P = 0.030$, $r^2 = 0.465$), which was lost when HN5 (exceptionally high EGFR) was excluded. No statistically significant correlations between Syk and β_1-integrin or between EGFR and β_1-integrin expression were found. Immunoprecipitation was carried out to investigate possible direct physical interactions between these proteins; HN6 cells were selected initially because they express all three proteins. Syk could be immunoprecipitated with EGFR (Fig. 1*D, top left*), however, no association between Syk and β_1 integrin was identified (data not shown). Coimmunoprecipitation between Syk or EGFR and GRB-2 was also detected, suggesting that these three proteins may form a signaling complex in SCCHN cells. The association between EGFR and Syk was confirmed in CAL 27 cells when EGFR was immunoprecipitated (Fig. 1*D, top right*) as well as in 011A cells transfected with Syk(L) (Fig. 1*D, bottom left*), but not in Syk-negative 011A parental cells (Fig. 1*D, bottom right*). EGFR was not generally detected in anti-Syk immunoprecipitates (except in HN6) probably because of the lower sensitivity of the Syk antibody as reported in similar studies (20).

To investigate any correlation between Syk expression and cell motility, three Syk-positive (CAL 27, HN5, and HN6) and three Syk-negative (006/1, 011A, and HN3) cell lines were tested in a Fluoroblok chemotaxis assay. No correlation between Syk expression and chemotactic ability was found because most cells actively migrated toward FCS (data not shown). To further study the role of Syk in cell motility, its expression and/or activity

was modified by overexpression, knockdown, or pharmacologic inhibition.

Syk overexpression increases chemotaxis of SIHN-011A cells. Syk-negative SIHN-011A cells were transfected with either pcDNA3.1-Syk(L) or pcDNA3.1-Syk(S). To confirm activity of the expressed protein, cell lysates were immunoprecipitated with Syk antibody and probed with phospho-Syk ($Tyr^{525/526}$) antibody or anti-phosphotyrosine antibody (4G10; Fig. 2*A*). Syk phosphorylation was observed in Syk(L)-expressing 011A cells in DMEM/10% FCS but not under serum-starved conditions. Growth rates of Syk(L), Syk(S), and Neo control clones were similar to the parental 011A cells (data not shown). Chemomigration was significantly enhanced (~70–80%) in Syk(L)-expressing clones compared with parental and Neo control cells. There was a slight increase in the number of migrating Syk(S)-expressing cells (~30–40%) but this did not achieve statistical significance (Fig. 2*B, left*).

Western blot analysis was done to investigate activation of specific proteins involved in migration (Fig. 2*B, right*). Increased levels of phosphorylated PLCγ1 were observed in Syk(L)- and (to a lesser extent) in Syk(S)-expressing 011A cells compared with controls. However, there was no obvious change in the (already high) level of phosphorylated AKT. Because Syk was shown to regulate urokinase-type plasminogen activator (uPA) secretion in breast cancer cells (27), uPA protein levels were investigated, but no differences were found between the various clones.

Syk inhibition reduces chemotaxis, Matrigel engagement, and haptotaxis of SCCHN cells. An siRNA approach was initially used to knock down Syk expression. Chemomigratory ability was significantly reduced in Syk siRNA–treated cells relative to inverted siRNA-treated control cells (Fig. 2*C, left*). However, the effect of Syk siRNA (20% inhibition) was less than that obtained with piceatannol (see below), possibly because of incomplete knockdown achieved by siRNA (Fig. 2*C, right*).

Piceatannol, a hydroxystilbene derivative of resveratrol, preferentially inhibits the activity of Syk in *in vitro* assays and is widely used as a Syk-selective inhibitor (28–30). Piceatannol was nontoxic to SCCHN cells at up to 100 μmol/L and we selected a concentration range commonly used in studies using human cells (14, 28–31). We confirmed that piceatannol inhibited Syk phosphorylation in HN6 cells at these concentrations (Supplementary Fig. S1). Piceatannol inhibited FCS-induced chemomigration of Syk-positive SCCHN cells (HN6 and CAL 27) in a concentration-dependent manner but had no significant effects in Syk-negative 011A cells (Fig. 2*D*).

Cell attachment and spreading on matrix proteins (primarily mediated via integrins) is a key early step in invasion. When cultured on Matrigel, many tumor cells attach and elongate, and

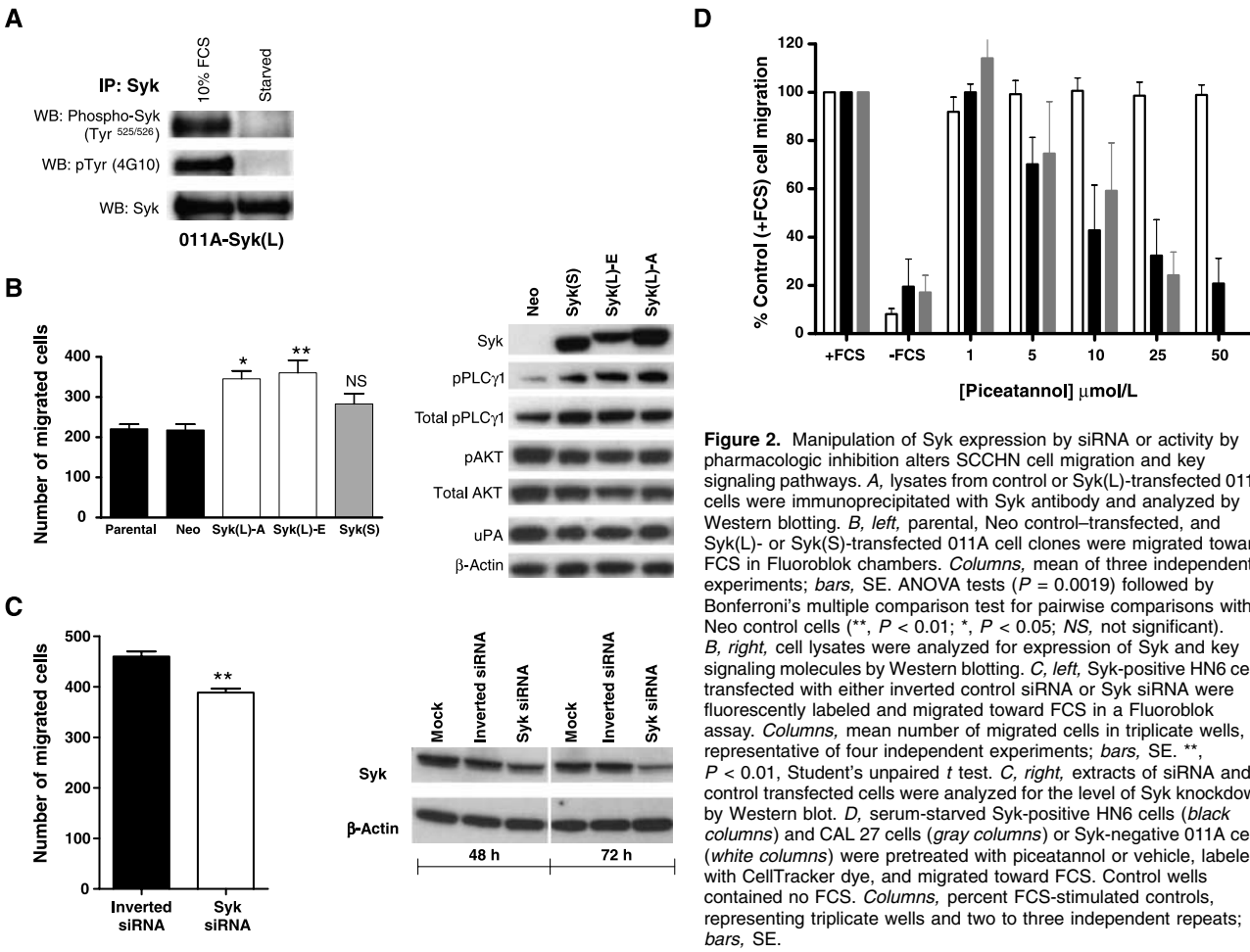

Figure 2. Manipulation of Syk expression by siRNA or activity by pharmacologic inhibition alters SCCHN cell migration and key signaling pathways. *A,* lysates from control or Syk(L)-transfected 011A cells were immunoprecipitated with Syk antibody and analyzed by Western blotting. *B, left,* parental, Neo control–transfected, and Syk(L)- or Syk(S)-transfected 011A cell clones were migrated toward FCS in Fluoroblok chambers. *Columns,* mean of three independent experiments; *bars,* SE. ANOVA tests ($P = 0.0019$) followed by Bonferroni's multiple comparison test for pairwise comparisons with Neo control cells (**, $P < 0.01$; *, $P < 0.05$; *NS,* not significant). *B, right,* cell lysates were analyzed for expression of Syk and key signaling molecules by Western blotting. *C, left,* Syk-positive HN6 cells transfected with either inverted control siRNA or Syk siRNA were fluorescently labeled and migrated toward FCS in a Fluoroblok assay. *Columns,* mean number of migrated cells in triplicate wells, representative of four independent experiments; *bars,* SE. **, $P < 0.01$, Student's unpaired *t* test. *C, right,* extracts of siRNA and control transfected cells were analyzed for the level of Syk knockdown by Western blot. *D,* serum-starved Syk-positive HN6 cells (*black columns*) and CAL 27 cells (*gray columns*) or Syk-negative 011A cells (*white columns*) were pretreated with piceatannol or vehicle, labeled with CellTracker dye, and migrated toward FCS. Control wells contained no FCS. *Columns,* percent FCS-stimulated controls, representing triplicate wells and two to three independent repeats; *bars,* SE.

this, together with motility, results in formation of cordlike structures and ultimately invasion. The ability of HN6 cells to form tubular networks on Matrigel was inhibited by piceatannol (Fig. 3*A*). A wider range of piceatannol concentrations was then tested in an assay using fluorescently labeled SCCHN cells, which enabled accurate quantification of tubularization on Matrigel by digital image analysis. Figure 3*B* shows that tube length was inhibited in a concentration-dependent manner in Syk-positive HN6 cells but not in Syk-negative 011A cells. In addition, piceatannol inhibited haptotactic motility of cells on collagen 1 (not shown) or on plastic in a scratch wound assay. Figure 3*C* shows a dose-dependent inhibition of wound closure using HN6 cells (with representative images shown in Fig. 3*D, top*). In contrast, Syk-negative 011A cells were able to complete wound closure at all doses tested (illustrated in Fig. 3*D, bottom*).

Key functional studies were repeated with a second Syk inhibitor, BAY 61-3606, an imidazopyrimidine compound reported to be a potent, ATP-competitive, reversible inhibitor of Syk tyrosine kinase activity with ~600-fold selectivity against Btk, Fyn, Itk, Lyn, and Src (32). This compound proved active in our cellular assays, significantly inhibiting chemomigration in Syk-positive cells (HN6 and CAL 27) but not in Syk-negative cells (011A; Supplementary Fig. S2*A*). It also inhibited HN6 tube formation on Matrigel (Supplementary Fig. S2*B* and *C*).

Signaling pathways associated with Syk activity in SCCHN cells. Western blot analysis was done on cells treated with piceatannol to investigate possible changes in the levels of phosphorylation of proteins involved in cell motility. A decrease in the level of phosphorylated AKT in piceatannol-treated HN6 cells was observed at 6 h and enhanced at 24 h, whereas no such change was observed in Syk-negative 011A cells. Levels of phosphorylated ERK were relatively unchanged (Fig. 4*A*). Similar results were obtained with BAY 61-3606 in HN6 cells (Supplementary Fig. S2*D*). It has been reported that Syk is able to phosphorylate PLCγ1 (22, 33); however, phosphorylated PLCγ1 was not detectable in either control or piceatannol-treated HN6 cells despite the presence of PLCγ1. We next measured calcium release (subsequent to PLCγ1 activation and opening of the endoplasmic inositol 1,4,5-trisphosphate–gated calcium channel) in Syk-positive CAL 27 cells in response to EGF stimulation and discovered that piceatannol was able to inhibit this process in a concentration-dependent fashion (Supplementary Fig. S3). Similar effects were seen with BAY 61-3606 (data not shown). Thus, a role for PLCγ1 in Syk-mediated SCCHN functions could be inferred from these observations.

Further Western blot analysis was carried out to explore whether the phenotypes observed in piceatannol treated HN6 cells were due to off-target effects on other proteins implicated in cell spreading. Focal adhesion kinase (FAK) and Src phosphorylation was not affected by piceatannol at the concentrations used (Fig. 4*B*). Although it is accepted that ancillary effects (independent of Syk) may contribute to the observed effects at higher concentrations of piceatannol, we believe that the additional studies with a pharmacologically distinct Syk inhibitor and the lack of effects of the two compounds in Syk-negative cells support a role for Syk in the functional assays utilized.

Syk is expressed in clinical SCCHN specimens and is associated with recurrence and/or reduced survival. First, the SYBR-based quantitative real-time PCR technique was used to detect mRNA levels of Syk in lesions from primary SCCHN (n = 38), nodal metastases (n = 14), and matched normal adjacent mucosae (n = 13) from Thai SCCHN patients. Syk expression in lymph nodes was significantly higher than in tumors and normal tissues (P = 0.045 and P = 0.011). The expression of Syk in tumors was also higher than in normal tissues although this did not achieve statistical significance (P = 0.084; Fig. 5*A*). Syk expression in primary SCCHN showed a statistically significant relationship with recurrence (Table 1). However, there was no association between Syk expression and age, gender, size of primary tumors, lymph node status, pathologic stage, or prior therapy in this relatively small study.

Lymphocytes and endothelial cells may contribute to the positive Syk signals in homogenized tumor samples assayed by real-time PCR and Western blots. To explore this possibility and also to acquire data on patients with a longer follow-up, a retrospective immunohistochemical analysis of primary tonsilar squamous cell carcinoma from UK patients (n = 38) was undertaken. Eight (21%) cancers showed strong Syk expression, 14 (37%) moderate, 10 (26%) weak, and 6 (16%) were negative. In stromal areas, focal Syk staining of leukocytes served as an internal positive control.

Whereas diffuse cytoplasmic staining for Syk was observed in the majority of the positive samples, additional focal nuclear staining of Syk was also observed in some samples, particularly in small tumor clusters (Fig. 5*B*). Different intensities and patterns of Syk staining were observed in the premalignant epithelial layers adjacent to invasive tumor lesions (Fig. 5*C*). It was also noted that Syk-negative epithelial layers appeared normal whereas those with Syk staining showed dysplasia. Tumor cells in the basal layer, in particular, the invasive edge, always showed stronger staining of Syk than those in the upper layers (Fig. 5*C*).

No statistically significant correlation was found between Syk expression and age, gender, size of primary tumors, lymph node status, pathologic stage, recurrence, or treatments (Supplementary Table S3). Nonetheless, there was an increased incidence of recurrence in the strong Syk-positive group (62.5%) compared with the moderate positive (35.7%), weak positive (30%), and negative (33%) groups.

For survival analysis, patients were divided into high Syk expression and lower Syk expression (low-moderate Syk staining and negative) groups. Survival was measured from diagnosis to the date of relapse/death or last follow-up. Survival curves and median survival times were calculated by the Kaplan-Meier method and groups compared by the log-rank test. Syk expression was significantly associated with worse survival (log rank, P = 0.002; Fig. 5*D*; Table 2). The mean survival period for the high Syk group was 18 months versus 95 months for the low Syk expression group. Recurrence rates also showed a significant correlation with worse survival (log rank, P < 0.001; Table 2). In contrast, other clinical variables including age, gender, size of primary tumors, lymph node status, pathologic stage, and postoperative treatment (in most cases radiotherapy) had no association with survival.

Discussion

Syk(L) and Syk(S) isoforms were identified in 6 of 10 SCCHN cell lines examined. In breast cancer cells, Syk expression was reported to correlate inversely with invasiveness (5). However, we found no such correlation in SCCHN cells as most of our cell lines showed strong migration toward 5% FCS. Syk(L) and Syk(S) were transfected into a Syk-negative cell line (SIHN-011A). Syk(L)-expressing cell migration was enhanced in a Fluoroblok transwell

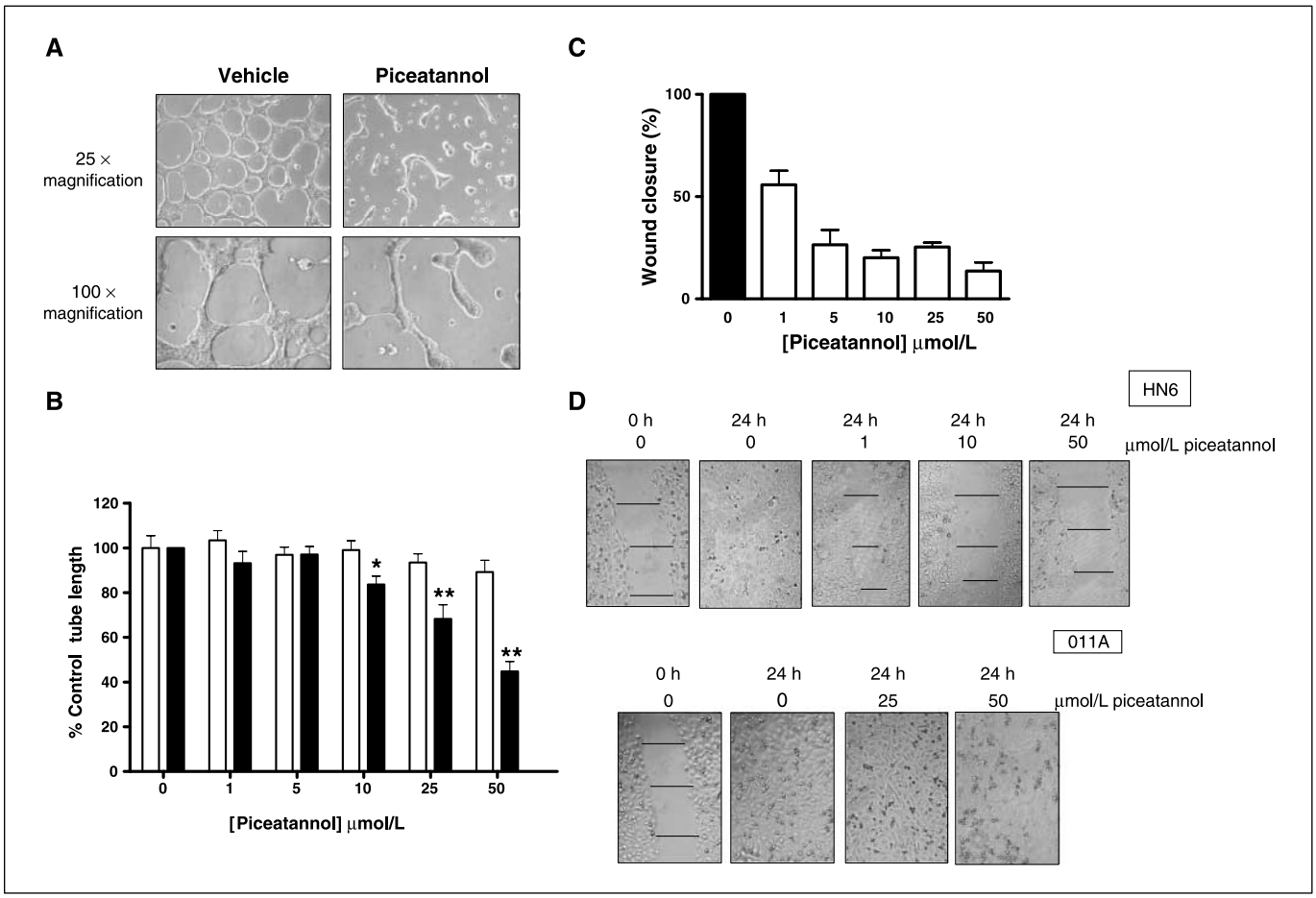

Figure 3. Syk inhibitors abrogate Matrigel engagement and haptotaxis of SCCHN cells. *A,* HN6 cells were seeded on Matrigel-coated wells with piceatannol (33 μmol/L) or vehicle and incubated overnight at 37°C. Morphology was observed by light microscopy. *B,* Syk-positive HN6 cells (*black columns*) or Syk-negative 011A cells (*white columns*) were treated with piceatannol or vehicle, labeled with CellTracker green dye, and seeded on Matrigel-coated wells. After 24 h, images were obtained and total tube length per field of view was measured using Image-Pro Plus software. Results ($n = 3$) are presented relative to vehicle control tube length. *, $P \leq 0.5$; **, $P \leq 0.01$. *C,* haptotaxis scratch wound assay. HN6 cells were seeded on 24-well plates and treated for 2 h with piceatannol or vehicle. A scratch wound was made and the degree of closure achieved after 24-h incubation was measured. *D, top,* representative images obtained from the HN6 haptotaxis assay; *bottom,* representative images from a parallel study done with Syk-negative 011A cells in which haptotaxis was not inhibited.

assay, possibly due to effects on cell plasticity and spreading. This could potentially be explained by the increased levels of phosphorylated PLCγ1 observed in Syk (L)-expressing cells (34). Interestingly, PLCγ1 activation was less marked in Syk(S)-expressing cells, and this may explain the weaker enhancement of chemomigration observed following transfection of this variant. In support of this, it was reported that Syk(S) has reduced ability to couple stimulation of immunoreceptors to intracellular

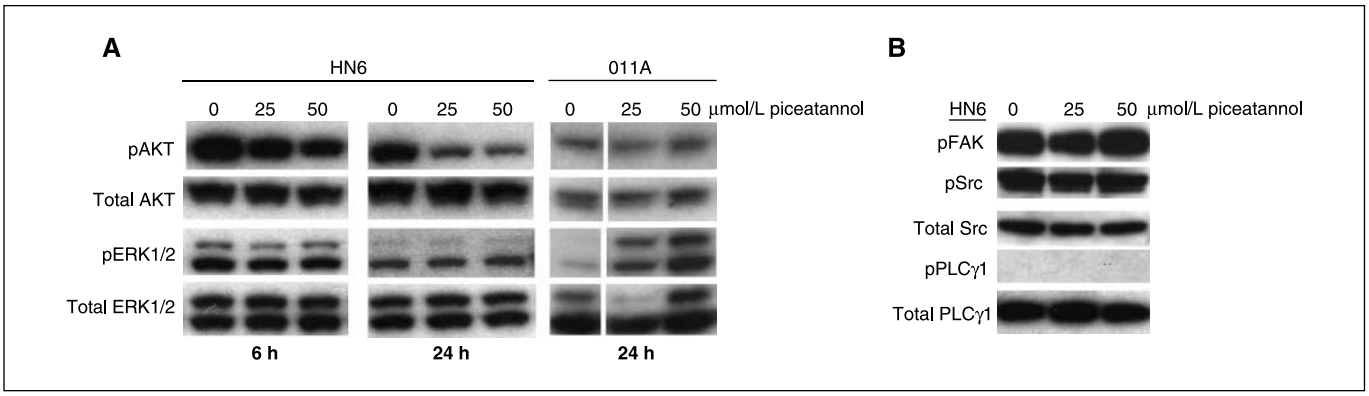

Figure 4. Piceatannol modulates activity of specific cell signaling proteins. *A,* Syk-positive HN6 cells or Syk-negative 011A cells were treated with piceatannol (25 or 50 μmol/L) or vehicle. Cell lysates were collected at 6 and/or 24 h and subjected to Western blot analysis for levels of phosphorylated or total AKT and ERK1/2. *B,* the levels of phosphorylated FAK, Src, and PLCγ1 were also investigated after 24-h piceatannol treatment of HN6 cells. Representative of two independent experiments.

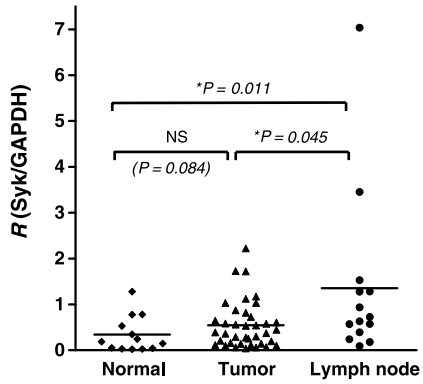

Sample	N	Sex (M/F)	R (Syk/GAPDH)		
			Mean	Median	Range
Normal	13	8:5	0.3436	0.1863	0.02 –1.28
1° Tumor	38	17:2	0.5440	0.3804	0.04 –2.22
Lymph node	14	8:6	1.3520	0.6792	0.09 –7.03

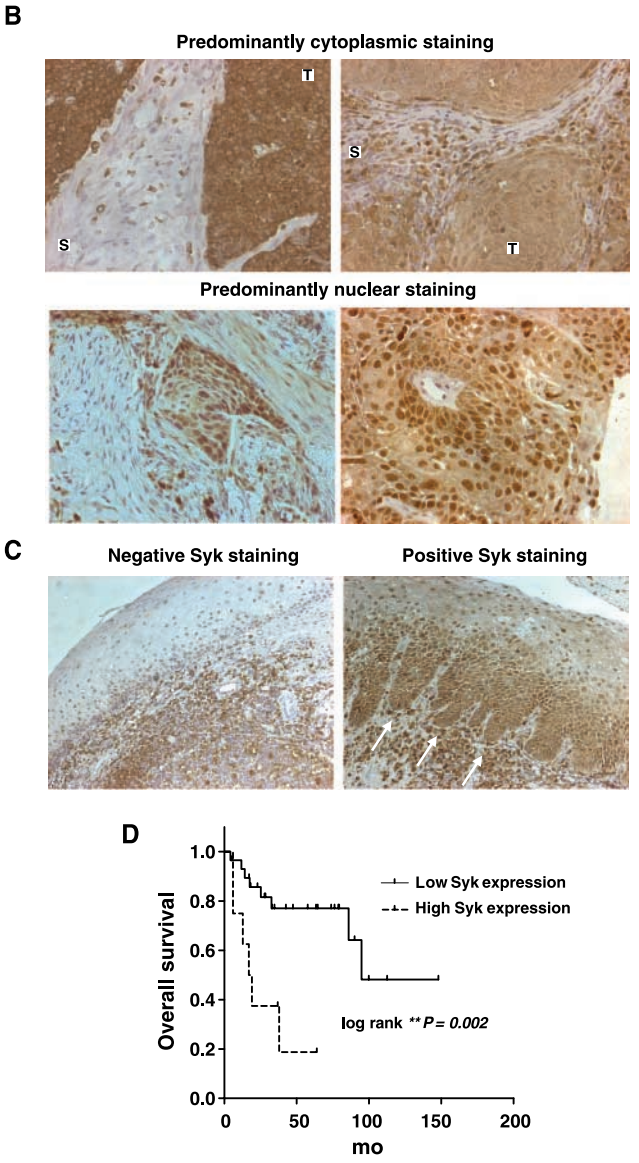

Figure 5. Syk expression in clinical SCCHN samples. *A,* levels of Syk expression in SCCHN patient samples by real-time PCR. Total RNA was extracted from tissue samples, converted to cDNA, and real-time PCR was done. The level of Syk expression (*R*) is expressed as a ratio compared with the calibrator sample using GAPDH as a reference. *, $P < 0.05$, Mann-Whitney U test; *NS,* not significant. Sample variables are tabulated (*bottom*). *B* and *C,* staining of Syk in SCCHN tumor tissues. Paraffin-embedded SCCHN tumor tissue sections were stained for Syk expression using monoclonal antibody (4D10). *B,* different patterns of Syk staining (predominantly cytoplasmic or nuclear) in tumor tissues (magnification, ×200). *T,* tumor; *S,* stroma. *C,* staining of Syk in SCCHN tissues: Syk-negative and Syk-positive epithelial layers (magnification, ×200). Note strong staining at invasive margin (*right, arrows*). *D,* Kaplan-Meier curves for the survival of patients with squamous cell carcinoma of the tonsil were calculated according to Syk expression (high versus low) as determined by immunohistochemistry. The two curves were compared using the log-rank test.

signaling pathways in basophils and B-cell and T-cell lines compared with Syk(L) (35).

Syk(S) lacks a 23-amino-acid sequence in the linker domain. In breast cancer, it was found that residues in the linker insert acted as a nuclear localization signal, which facilitated the nuclear transport of Syk(L), but Syk(S) located exclusively in the cytoplasm (25). However, Syk(L) and Syk(S) were present in both nuclei and cytoplasm in our transfected 011A cells (not shown). This is consistent with observations by Zhou et al. (36) in B lymphocytes and breast cancer cells. Syk(S) expression was detected by RT-PCR or Western blot in all six Syk-positive cell lines in this study and its expression was usually lower than Syk(L). Immunohistochemistry can clarify the localization of Syk expression in tumors but it cannot be used to discriminate the specific isoforms because there are no selective antibodies available. Wang et al. (25) observed that Syk(S) expression occurred frequently in primary breast tumors but not in matched normal mammary tissues, suggesting a contribution of Syk(S) to mammary tumor progression. To investigate this, RT-PCR using a primer pair that can detect both Syk(L) and Syk(S) was done in clinical SCCHN samples to see whether there is a similar pattern. However, Syk(S) was detected in both normal and tumor tissue samples (data not shown).

To complement these studies, the effect of Syk inhibition on SCCHN cell functions was explored. Syk inhibitors piceatannol and BAY 61-3606 induced a dose-dependent inhibition of interconnecting networks of HN6 cells (but not of Syk-negative 011A cells) on Matrigel. Similar inhibitory effects of these compounds were seen in haptotaxis and chemotaxis assays, which might mimic key aspects of cell invasion and metastasis. We also showed that siRNA targeting Syk inhibited chemotaxis, although to a lesser degree, possibly due to incomplete knockdown of protein expression. These data are consistent with previous studies in endothelial cells (6), nasopharyngeal cells (15), and aortic smooth muscle cells (37), implicating Syk in cell migration.

Table 1. Relationship between Syk mRNA expression and clinicopathologic characteristics in 38 Thai SCCHN tumor tissue samples

Characteristics	*n* (%)	Syk expression		
		Low (<Q3)	High (≥Q3)	*P*
		n	*n*	
Age (y)				
<65	15 (39)	11	4	1.000
≥65	23 (61)	17	6	
Gender				
Male	17 (45)	12	5	0.727
Female	21 (55)	16	5	
T classification				
T_{1-2}	15 (39)	10	5	0.473
T_{3-4}	23 (61)	18	5	
Lymph node involvement				
Negative	23 (61)	15	8	0.259
Positive	15 (39)	13	2	
Pathologic stage				
I-II	10 (26)	5	5	0.090
III-IV	28 (74)	23	5	
Recurrence				
No	19 (50)	18	1	0.008
Yes	19 (50)	10	9	
Prior radiotherapy or chemoradiotherapy				
No	29 (76)	24	5	0.064
Radiotherapy	6 (16)	3	3	
Chemoradiotherapy	3 (8)	1	2	

We next carried out preliminary studies to explore possible underlying mechanisms and reported for the first time an association between Syk and EGFR in SCCHN cells, as previously described in breast epithelial cells (20). Thus, Syk might act downstream of EGFR and could be partially responsible for the inhibitory effects on chemotaxis observed in piceatannol- and BAY 61-3606–treated SCCHN cells, although these results are the converse of those reported in breast cancer cells. Previous studies have also suggested Syk involvement in integrin signaling in platelets and airway epithelial cells (14, 38) but we found no direct association between Syk and β_1 integrin in SCCHN cells. This could be because their interaction, if present, is transient or not stable under the conditions used.

Table 2. Relationship between Syk immunostaining or clinicopathologic characteristics and survival in 38 UK patients with squamous cell carcinoma of the tonsil

Variables	Survival (*P*)
Age (≤60 vs >60 y)	0.161
Gender	0.338
T stage (T_{1-2} vs T_{3-4})	0.524
Lymph node status	0.707
Pathologic stage (I, II vs III, IV)	0.325
Recurrence	<0.001
Syk staining	0.002
Postoperative treatment	0.652

Western blot analysis of piceatannol- and BAY 61-3606–treated cell lysates indicated a decrease in phosphorylated AKT, which may imply the involvement of PI3K, a pivotal molecule implicated in migration and chemotaxis of both tumor and endothelial cells (39). Phosphorylation of Syk at Tyr^{323} forms a docking site for the p85 subunit of PI3K (21). Interactions between Syk and PI3K were reported in natural killer cells (40) and PI3K is required for the EGF-induced migration, which is mediated by the up-regulation of β_1 integrin in breast cancer cells (41). However, ERK and p38 mitogen-activated protein kinase were implicated in platelet-derived growth factor (PDGF)-BB–mediated migration in rat aortic smooth muscle cells (37). Syk clearly interacts with multiple downstream pathways and responses may depend on the types and relative levels or activation of receptor tyrosine kinase (RTK) and integrins in different cell types.

Both PI3K and PLCγ1 signaling contribute to cell motility in response to RTK and integrin activation. PLCγ1 is suggested as an additional downstream target of Syk because increased levels of phosphorylated PLCγ1 were observed in Syk(L)-overexpressing 011A cells and piceatannol inhibited EGF-stimulated calcium release, putatively via PLCγ1 and inositol 1,4,5-trisphosphate. Moreover, Syk is reported to directly phosphorylate PLCγ1 (22, 33). Taken together, our data suggest the possibility that Syk is involved in coordinated cell signaling, whereby, together with GRB-2, it could act downstream of EGFR and integrins, converging both of these environment-sensing input signals to downstream effectors including the PI3K/AKT and PLCγ pathways.

Pilot investigations into Syk expression in clinical SCCHN specimens and their relationship to clinical variables were

undertaken in two independent patient cohorts. Syk mRNA expression in lymph node metastases was significantly higher than in primary tumors and normal tissues. In addition, there seemed to be a higher Syk expression in tumors relative to normal tissues, although this was not statistically significant. Immunohistochemical analysis of a different (archival) set of primary tumors was then used to identify whether Syk expression is primarily epithelial or stromal. Syk expression was observed in 84% of the primary tumors. Although varying levels of positive staining of leukocytes were found in stromal areas (possibly depending on the degree of inflammation), the staining was not prominent and unlikely to be a major contributor to the total levels detected in homogenized tumor tissues.

Analysis of clinical variables and Syk expression in primary tumors showed a possible association of Syk expression with recurrence but not with other features including lymph node status. Survival analysis of patients in the retrospective immunohistochemical study showed that high Syk expression correlated with worse survival and thus might be useful as a prognostic indicator in SCCHN. However, this would need to be confirmed in a larger series. The present results contrast with those reported in breast cancer (42–44) or gastric cancer (45), which showed decreased Syk expression in invasive carcinoma. Syk may have different roles in different types of cells and/or cancer cells: whereas the majority of head and neck cancers are squamous, breast and gastric cancers are primarily adenocarcinomas. In normal gastric epithelium, Syk staining was predominantly nuclear and scanty in cytoplasm (45); in normal breast tissue and benign lesions, Syk staining was cytoplasmic (42).

Oral mucosae from noncancer patients were not available in the present studies, but Syk was not expressed in histologically normal epithelia distant from the tumor and, in contrast, predominantly nuclear Syk staining was observed in dysplastic epithelial cells adjacent to tumors. Stronger, predominately nuclear staining of Syk was particularly observed at the invasive front of dysplastic epithelial layers whereas weaker cytoplasmic staining of Syk was detected in the normal epithelial layers. It is possible that differential expression of Syk(L) and its splice variant Syk(S) may contribute to the disparate observations in different cancers. In human breast, Syk(S) was reported to be expressed in carcinomas but not in matched normal mammary tissues, suggesting a contribution of Syk(S) to mammary tumor progression (25). In contrast, in SCCHN, Syk(S) expression was detected in both tumor and normal tissues by RT-PCR. Future development of isoform-specific Syk antibodies may help to determine whether there are differences in the expression and localization of Syk isoforms in different cancer types and their corresponding normal tissues. Only with more precise determination of these factors will a clear evaluation of the possible contribution of Syk to tumor progression be possible.

Acknowledgments

Received 1/25/2007; revised 5/25/2007; accepted 6/4/2007.

Grant support: Head and Neck Cancer Research Trust, Royal Marsden Hospital, UK and The Medical Scholars Program, Mahidol University, Thailand.

The costs of publication of this article were defrayed in part by the payment of page charges. This article must therefore be hereby marked *advertisement* in accordance with 18 U.S.C. Section 1734 solely to indicate this fact.

We thank Dr. Jiale Dai (Department of Molecular Pathology, M. D. Anderson Cancer Center, Houston, TX) for providing Syk(L) and Syk(S) plasmids. We also thank Dr. Philip Wilson (Consultant Histopathologist, St. George's Hospital, London, United Kingdom) for providing clinical samples. We are grateful to Zai Ahmad and Sharon Gowan for their expert advice and assistance.

References

1. Turner M, Schweighoffer E, Colucci F, Di Santo JP, Tybulewicz VL. Tyrosine kinase SYK: essential functions for immunoreceptor signalling. Immunol Today 2000;21:148–54.
2. Wang H, Malbon CC. G(s)α repression of adipogenesis via Syk. J Biol Chem 1999;274:32159–66.
3. Yamada T, Fujieda S, Yanagi S, et al. Protein-tyrosine kinase Syk expressed in human nasal fibroblasts and its effect on RANTES production. J Immunol 2001;166:538–43.
4. Fluck M, Zurcher G, Andres AC, Ziemiecki A. Molecular characterization of the murine syk protein tyrosine kinase cDNA, transcripts and protein. Biochem Biophys Res Commun 1995;213:273–81.
5. Coopman PJ, Do MT, Barth M, et al. The Syk tyrosine kinase suppresses malignant growth of human breast cancer cells. Nature 2000;406:742–7.
6. Inatome R, Yanagi S, Takano T, Yamamura H. A critical role for Syk in endothelial cell proliferation and migration. Biochem Biophys Res Commun 2001;286:195–9.
7. Yanagi S, Inatome R, Ding J, Kitaguchi H, Tybulewicz VL, Yamamura H. Syk expression in endothelial cells and their morphologic defects in embryonic Syk-deficient mice. Blood 2001;98:2869–71.
8. Yanagi S, Inatome R, Takano T, Yamamura H. Syk expression and novel function in a wide variety of tissues. Biochem Biophys Res Commun 2001;288:495–8.
9. Bolen JB. Protein tyrosine kinases in the initiation of antigen receptor signaling. Curr Opin Immunol 1995;7:306–11.
10. Sada K, Takano T, Yanagi S, Yamamura H. Structure and function of Syk protein-tyrosine kinase. J Biochem (Tokyo) 2001;130:177–86.
11. Siraganian RP, Zhang J, Suzuki K, Sada K. Protein tyrosine kinase Syk in mast cell signaling. Mol Immunol 2002;38:1229–33.
12. Zhang J, Berenstein EH, Evans RL, Siraganian RP. Transfection of Syk protein tyrosine kinase reconstitutes high affinity IgE receptor-mediated degranulation in a Syk-negative variant of rat basophilic leukemia RBL-2H3 cells. J Exp Med 1996;184:71–9.
13. Obergfell A, Eto K, Mocsai A, et al. Coordinate interactions of Csk, Src, and Syk kinases with αIIbβ3 initiate integrin signaling to the cytoskeleton. J Cell Biol 2002;157:265–75.
14. Ulanova M, Marcet-Palacios M, Munoz S, et al. Involvement of Syk kinase in TNF-induced nitric oxide production by airway epithelial cells. Biochem Biophys Res Commun 2006;351:431–7.
15. Lu J, Lin WH, Chen SY, et al. Syk tyrosine kinase mediates Epstein-Barr virus latent membrane protein 2A-induced cell migration in epithelial cells. J Biol Chem 2006;281:8806–14.
16. Rogers SJ, Harrington KJ, Rhys-Evans P, O-charoenrat P, Eccles SA. Biological significance of c-erbB family oncogenes in head and neck cancer. Cancer Metastasis Rev 2005;24:47–69.
17. Grandis JR, Tweardy DJ. Elevated levels of transforming growth factor α and epidermal growth factor receptor messenger RNA are early markers of carcinogenesis in head and neck cancer. Cancer Res 1993;53:3579–84.
18. Brandt BH, Roetger A, Dittmar T, et al. c-erbB-2/EGFR as dominant heterodimerization partners determine a mitogenic phenotype in human breast cancer cells. FASEB J 1999;13:1939–49.
19. Eccles SA. Targeting key steps in metastatic tumour progression. Curr Opin Genet Dev 2005;15:77–86.
20. Ruschel A, Ullrich A. Protein tyrosine kinase Syk modulates EGFR signalling in human mammary epithelial cells. Cell Signal 2004;16:1249–61.
21. Moon KD, Post CB, Durden DL, et al. Molecular basis for a direct interaction between the Syk protein-tyrosine kinase and phosphoinositide 3-kinase. J Biol Chem 2005;280:1543–51.
22. Law CL, Chandran KA, Sidorenko SP, Clark EA. Phospholipase C-γ1 interacts with conserved phosphotyrosyl residues in the linker region of Syk and is a substrate for Syk. Mol Cell Biol 1996;16:1305–15.
23. O-charoenrat P, Modjtahedi H, Rhys-Evans P, Court WJ, Box GM, Eccles SA. Epidermal growth factor-like ligands differentially up-regulate matrix metalloproteinase 9 in head and neck squamous carcinoma cells. Cancer Res 2000;60:1121–8.
24. O-charoenrat P, Rhys-Evans P, Eccles SA. Expression of vascular endothelial growth factor family members in head and neck squamous cell carcinoma correlates with lymph node metastasis. Cancer 2001;92:556–8.
25. Wang L, Duke L, Zhang PS, et al. Alternative splicing disrupts a nuclear localization signal in spleen tyrosine kinase that is required for invasion suppression in breast cancer. Cancer Res 2003;63:4724–30.
26. Niinaka Y, Haga A, Raz A. Quantification of cell motility: gold colloidal phagokinetic track assay and wound healing assay. Methods Mol Med 2001;58:55–60.
27. Mahabeleshwar GH, Kundu GC. Syk, a protein-tyrosine kinase, suppresses the cell motility and nuclear factor κB-mediated secretion of urokinase type plasminogen activator by inhibiting the phosphatidylinositol 3′-kinase activity in breast cancer cells. J Biol Chem 2003;278:6209–21.
28. Leseux L, Hamdi SM, Al Saati T, et al. Syk-dependent mTOR activation in follicular lymphoma cells. Blood 2006;108:4156–62.
29. Oliver JM, Burg DL, Wilson BS, McLaughlin JL,

Geahlen RL. Inhibition of mast cell Fc epsilon R1-mediated signaling and effector function by the Syk-selective inhibitor, piceatannol. J Biol Chem 1994;269:29697–703.
30. Rinaldi A, Kwee I, Taborelli M, et al. Genomic and expression profiling identifies the B-cell associated tyrosine kinase Syk as a possible therapeutic target in mantle cell lymphoma. Br J Haematol 2006;132:303–16.
31. Keely PJ, Parise LV. The $\alpha_2\beta_1$ integrin is a necessary co-receptor for collagen-induced activation of Syk and the subsequent phosphorylation of phospholipase Cγ2 in platelets. J Biol Chem 1996;271:26668–76.
32. Yamamoto N, Takeshita K, Shichijo M, et al. The orally available spleen tyrosine kinase inhibitor 2-[7-(3,4-dimethoxyphenyl)-imidazo[1,2-c]pyrimidin-5-ylamino]-nicotinamide dihydrochloride (BAY 61-3606) blocks antigen-induced airway inflammation in rodents. J Pharmacol Exp Ther 2003;306:1174–81.
33. Rodriguez R, Matsuda M, Perisic O, et al. Tyrosine residues in phospholipase Cγ2 essential for the enzyme function in B-cell signaling. J Biol Chem 2001;276:47982–92.
34. Jones NP, Peak J, Brader S, Eccles SA, Katan M. PLCγ1 is essential for early events in integrin signalling required for cell motility. J Cell Sci 2005;118:2695–706.
35. Latour S, Zhang J, Siraganian RP, Veillette A. A unique insert in the linker domain of Syk is necessary for its function in immunoreceptor signalling. EMBO J 1998;17:2584–95.
36. Zhou F, Hu J, Ma H, Harrison ML, Geahlen RL. Nucleocytoplasmic trafficking of the Syk protein tyrosine kinase. Mol Cell Biol 2006;26:3478–91.
37. Lee CK, Lee HM, Kim HJ, et al. Syk contributes to PDGF-BB-mediated migration of rat aortic smooth muscle cells via MAPK pathways. Cardiovasc Res 2007;74:159–68.
38. Willeke T, Schymeinsky J, Prange P, Zahler S, Walzog B. A role for Syk-kinase in the control of the binding cycle of the β_2 integrins (CD11/CD18) in human polymorphonuclear neutrophils. J Leukoc Biol 2003;74:260–9.
39. Brader S, Eccles SA. Phosphoinositide 3-kinase signalling pathways in tumor progression, invasion and angiogenesis. Tumori 2004;90:2–8.
40. Jiang K, Zhong B, Ritchey C, et al. Regulation of Akt-dependent cell survival by Syk and Rac. Blood 2003;101:236–44.
41. Adelsman MA, McCarthy JB, Shimizu Y. Stimulation of β_1-integrin function by epidermal growth factor and heregulin-β has distinct requirements for erbB2 but a similar dependence on phosphoinositide 3-OH kinase. Mol Biol Cell 1999;10:2861–78.
42. Dejmek J, Leandersson K, Manjer J, et al. Expression and signaling activity of Wnt-5a/discoidin domain receptor-1 and Syk plays distinct but decisive roles in breast cancer patient survival. Clin Cancer Res 2005;11:520–8.
43. Moroni M, Soldatenkov V, Zhang L, et al. Progressive loss of Syk and abnormal proliferation in breast cancer cells. Cancer Res 2004;64:7346–54.
44. Toyama T, Iwase H, Yamashita H, et al. Reduced expression of the Syk gene is correlated with poor prognosis in human breast cancer. Cancer Lett 2003;189:97–102.
45. Nakashima H, Natsugoe S, Ishigami S, et al. Clinical significance of nuclear expression of spleen tyrosine kinase (Syk) in gastric cancer. Cancer Lett 2006;236:89–94.

Syk Tyrosine Kinase Is Linked to Cell Motility and Progression in Squamous Cell Carcinomas of the Head and Neck

Sutima Luangdilok, Carol Box, Lisa Patterson, et al.

Cancer Res 2007;67:7907-7916.